ISSN 2250-3153

A Synchronous Cuk Converter Based Photovoltaic Energy System Design and Simulation

K.Kavitha[*], Dr. Ebenezer Jeyakumar[**]

[*] Department of ECE, Vivekanandha Institute of Engineering and Technology for Women, Tiruchengode, Tamilnadu, India
[**] Director (Academics), Sri Ramakrishna Engineering College, Ciombatore, Tamilnadu, India

Abstract- In this paper, a synchronous cuk converter proposed for analyzing the performance of photovoltaic system is presented. In the proposed cuk converter, the conduction losses and switching losses are reduced. The conduction losses are reduced by replacing the diode with MOSFET and the switching losses are reduced by providing an auxiliary circuit. The proposed converter system is operated based on the soft switching techniques. These switching techniques are to provide smooth transition of voltage and current. So, the conversion efficiency of the PV system is improved and the load meeting the dynamic energy requirement is in an efficient way. It has a significant advantage over other inverting topologies since they enable low voltage ripple on both the input and the output sides of the converter. Then, the different operation mode of proposed synchronous cuk converter is analyzed at different operating condition of auxiliary and main circuit. From the operating mode, the output current of each modes are determined. The proposed synchronous cuk converter implemented in MATLAB simulation platform and the output performance is analyzed.

Index Terms- cuk converter, synchronous cuk converter, photovoltaic system, MOSFET, auxiliary and main circuit.

I. INTRODUCTION

Renewable sources of energy acquire growing importance due to massive consumption and exhaustion of fossil fuel [4] [11] [12]. Generally, solar energy conversion systems can be classified into two categories: thermal systems which convert solar energy into heat and photovoltaic systems which convert solar energy to electricity [3]. Among several renewable energy sources, Photovoltaic arrays are used in many applications such as water pumping, battery charging, hybrid vehicles, and grid connected PV systems [5]. Photovoltaic system is the direct conversion of sunlight to electricity [1]. They are highly reliable and constitute a nonpolluting source of electricity, which can be appropriate for many applications [2].

For storage or other DC components to be used in conjunction with AC loads, some type of power conversion capability is required [6]. Considering that the output characteristic of a photovoltaic cell has a wide voltage range, depending on the operating conditions of a photovoltaic cell, the DC/DC converter needs to have a wide input voltage range to regulate the constant output voltage [7]. To achieve high step-up and high efficiency DC/DC converters is the major consideration in the renewable power applications due to the low voltage of PV arrays and fuel cells [10] [14]. The purpose of dc-dc converter is insure the impedance adaptation between the PV source generation and the main utility by tracking the reference voltage required by the grid [9]. The DC-DC converter converts a DC input voltage, to a DC output voltage, with a magnitude lower or higher than the input voltage [8] [15] [17].

There are several different types of dc-dc converters, buck, boost, buck-boost and cuk topologies, have been developed and reported in the literature to meet variety of application specific demands. One advantage of these converters has high power efficiency [13] [16] [18]. Higher order dc-dc converters, such as the cuk converter, have a significant advantage over other inverting topologies since they enable low voltage ripple on both the input and the output sides of the converter [19]. As with other DC-DC converters the cuk converter can either operate in continuous or discontinuous current mode. However, unlike these converters, it can also operate in discontinuous voltage mode [20].

In this paper, a synchronous DC-DC cuk converter design and implement for photovoltaic application. The proposed synchronous cuk converter has a significant advantage over other inverting topologies since they enable low voltage ripple on both the input and the output sides of the converter. So, the performance of photovoltaic system and the output efficiency of converter is improved. The circuit diagram of synchronous cuk converter and the different mode of operation are described in section 3. Prior to that, the recent research works are given in section 2. In section 4, the results and discussion of synchronous converter based PV system are described. The section 5 concludes the paper.

II. RECENT RESEARCH WORKS: A BRIEF REVIEW

Numerous related research works are already existed in literature which based on DC-DC converter PV system. Some of them reviewed here.

Yu Kang Lo et al. [21] has presented a photovoltaic (PV) system parallel connected to an electric power grid with a power factor corrector (PFC) for supplying the dc loads. The operation principles and design considerations for the presented PV system were analyzed and discussed. The balanced distribution of the power flows between the utility and the PV panels was achieved automatically by regulating the output dc voltage of the PFC. Experimental results were shown to verify the feasibility of the proposed topology, which could effectively transfer the tracked maximum power from the PV system to the dc load, while the unity power factor was obtained at the utility side.

Ho-sung Kim et al. [22] has discussed that the photovoltaic (PV) power conditioning system (PCS) must have high

conversion efficiency and low cost. Generally, a PV PCS uses either a single string converter or a multilevel module integrated converter (MIC). Each of these approaches has both advantages and disadvantages. For a high conversion efficiency and low cost PV module, a series connection of a module integrated DC–DC converter output with a photovoltaic panel was proposed. The output voltage of the PV panel was connected to the output capacitor of the fly-back converter. Thus, the converter output voltage was added to the output voltage of the PV panel. The isolated DC–DC converter generates only the difference voltage between the PV panel voltage and the required total output voltage. This method reduces the power level of the DC–DC converter and enhances energy conversion efficiency compared with a conventional DC–DC converter.

Athimulam Kalirasu et al. [23] has presented simulation of open loop and closed loop controlled boost converter system for solar installation system. MATLAB models for open loop and closed loop systems were developed using the blocks of simulink and the same are used for simulation studies. The closed loop system was able to maintain constant voltage. These converters have advantages like reduced hardware and good output voltage regulation. Thus the boost converter was capable of improving the voltage level from 15 V to the required level.

Arun K. Verma et al. [24] has investigated the solar power generation isolated portable system using a boost converter and a single stage sine wave boost inverter. The proposed configuration boosts the low voltage of photovoltaic (PV) array using a dc-dc boost converter to charge the battery at 96V and to convert this battery voltage into high quality 230V rms ac voltage at 50Hz for feeding autonomous loads without any intermediate conversion stage and a filter. A maximum power point tracking (MPPT) scheme was proposed with series connection of a dc–dc converter input with a PV panel for high efficiency.

M. Vaigundamoorthi et al. [25] has analyzed and designed the high efficient modified soft controlled (ZVS-PWM) Active-Clamping Cuk (buck- boost type) converter to extract maximum power from solar Photo Voltaic (PV) module. The solar PV module, Maximum Power Point Tracking (MPPT), ZVS based Cuk converter have been modeled and simulated in MATLAB/Simulink. Using Perturb and Observer (PAO) algorithm, the maximum power was tracked from solar PV module. In order to reduce the switching losses across the switches, the soft switching has been implemented for all the three active switches of modified Cuk converter, resulting in high conversion efficiency at high-frequency operation, improved transient, and steady state response without significant increase in voltage and current stresses on switches.

A.Kalirasu et al. [26] has presented simulation of open loop and closed loop controlled buck converter system for solar installation system. MATLAB models for open loop and closed loop systems are developed using the blocks of simulink and the same are used for simulation studies. The closed loop system is able to maintain constant voltage. This converter has advantages like reduced hardware and good output voltage regulation. The simulation results are in line with the theoretical predictions.

W.M.Utomo et al. [27] has proposed a neural network control scheme of a DC-DC Buck-Boost converter to produce variable DC voltage source that would be applied on DC motor drives. In this technique, a back propagation learning algorithm was derived. The controller was designed to track the output voltage of the DC-DC converter and to improve performance of the Buck-Boost converter during transient operations. Furthermore, to investigate the effectiveness of the proposed controller, some operations such as starting-up and reference voltage variations were verified.

The review of the recent research works reveals that, the DC-DC converter based photo voltaic (PV) energy system is applied various convenient applications. It converts one DC voltage level to another, by storing the input energy temporarily and then releasing that energy to the output at a different voltage. In the time of conversion process, the MOSFET switching frequency is increased so switching power loss is occurred. Therefore, the switching driver circuit is needed for driving the device without switching losses. In recently, the synchronous buck converter is used to reduce the switching loss in the main MOSFET over conventional dc-dc buck converter. The drawbacks of synchronous buck converter is that it converts only the limited range voltage, so it can be used only for low switching frequency applications. Also, in higher order application, the converter topologies have the disadvantage that the high voltage ripples are present on both the input and the output sides of the converter. Thus, a soft switching based converter is required for reducing the power loss.

To overcome this problem, in this paper a synchronous cuk converter based PV system is proposed. The proposed cuk converter improves the performance of PV system so that the converter performance is also improved. In the proposed converter, the conduction loss is to be reduced by replacing the diode with MOSFET, but also switching losses is reduced by providing an auxiliary circuit. The proposed converter system is operated based on the soft switching techniques. These switching techniques are used to provide for smooth transition of voltage and current. So, the conversion efficiency of the PV system is improved and the load meeting the dynamic energy requirement is in an efficient way. The proposed synchronous cuk converter is have a significant advantage over other inverting topologies since they enable low voltage ripple on both the input and the output sides of the converter.

III. Proposed Synchronous Cuk Converter

The proposed synchronous cuk converter is the extension of classical converter but, for making the synchronous operation, the auxiliary circuit is added. The structure of proposed synchronous cuk converter is illustrated in figure 1. In the proposed cuk converter, the input side and output side inductors are denoted as L_1 and L_2 respectively. The output capacitor and inductor acts as filter circuit providing only the DC component and filtering the AC component. Here, three MOSFETs are used as main switch as well as auxiliary switches which are denoted as S, S_1 and S_2. The auxiliary switches S_1 and S_2 are parallel with the main switch. The resonant capacitor and resonant inductor are denoted as C_r and L_r. The resonant capacitor is charged at normal operation and it

discharges the voltage during abnormal operation and the diode is conducted. The resonant capacitor is providing the time delay and to minimize the switching losses of converter. So this synchronous converter can be used for high as well as low switching frequencies. The output voltage, current, resistance and capacitor are denoted as $V_o, I_o, R_o \text{ and } C_o$ respectively. Then, the current capacitor across the main circuit is denoted as C_r. The resistance across the MOSFETs $S, S_1 \text{ and } S_2$ are denoted as $r_o, r_{o(1)} \text{ and } r_{o(2)}$ respectively. The proposed cuk converter circuit L_1 gram is given as follo C_S them. L_2

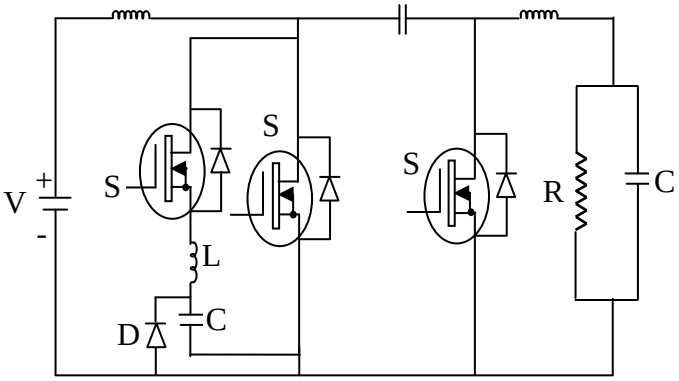

Figure 1: Structure of Proposed Synchronous Cuk Converter.

From the above diagram, the main switch and auxiliary switch are not subjected to additional voltage stresses but the main switch has more current stress in comparison to the auxiliary one. The output inductor is chosen such that the output current is kept constant and the output capacitor is chosen in such a way that the output voltage remains constant and ripple free as well. The resonant capacitor and resonant inductor are calculated as following formula.

$$C_r = \frac{I_{in(max)} T_D (a-1)^2}{V_o\left(1+\frac{\pi(a-1)}{2}\right)} \quad (1)$$

$$L_r = \frac{V_o T_D}{I_{in(max)}\left(1+\frac{\pi(a-1)}{2}\right)} \quad (2)$$

Where, T_D is the delay time and a is the stress factor. Then, the above circuit is converted into equivalent circuit model and from the model, the output current is calculated by following formula.

$$I_o = I_s - \frac{1}{V_s}\left(r_o + r_{o(1)} + r_{o(2)} + j\omega L_r + \frac{1}{j\omega}.\left(\frac{1}{C_r}+\frac{1}{C_s}\right)\right) \quad (3)$$

Then, the values of resonant capacitor and resonant inductor are substituted in equation (3), and the modified equation is given as following formula.

$$I_o = I_s - \frac{1}{V_s}\left(r_o + r_{o(1)} + r_{o(2)} + j\omega\left(\frac{V_o T_D}{I_{in(max)}\left(1+\frac{\pi(a-1)}{2}\right)}\right) + \frac{1}{j\omega}\left(\frac{\left(V_o\left(1+\frac{\pi(a-1)}{2}\right)\right)}{I_{in(max)} T_D (a-1)^2} + \frac{1}{C_s}\right)\right) \quad (4)$$

The output resistance of MOSFET is varied in two different operating points. The two operating points are linear and saturation. In these two different operating points, the output resistance values are tabulated as follows.

Table I: MOSFET Output Resistance.

Operating Points	r_o	$r_{o(1)}$	$r_{o(2)}$
Linear	$\frac{1}{K(V_{GS}-V_S)}$	$\frac{1}{K_{(1)}(V_{GS(1)}-V_S)}$	$\frac{1}{K_{(2)}(V_{GS(2)}-V_S)}$
Saturation	$\frac{1}{K(V_{GS}-V_S)\lambda}$	$\frac{1}{K_{(1)}(V_{GS(1)}-V_S)\lambda_{(1)}}$	$\frac{1}{K_{(2)}(V_{GS(2)}-V_S)\lambda_{(2)}}$

3.1. Different Operating Modes of Proposed Synchronous Cuk Converter

The different operating modes are derived from the equivalent circuit model of synchronous cuk converter. The operating modes are based on zero-voltage switching (ZVS) and zero-current switching (ZCS). These operating modes are selected by the main and auxiliary MOSFET switching. As per the operation of main and auxiliary circuit, the operating modes of synchronous cuk converter are categorized into eight modes. The circuit diagrams of eight modes are illustrated as follows.

Mode I:

In the mode I operation, the main circuit MOSFET is ZVS and the auxiliary circuit MOSFET S_2 is also ZVS. But, in the second auxiliary circuit, the MOSFET diode is only ZCS. Then, in mode I, the resonant capacitor C_r and resonant inductor L_r are conducted. The mode I operation equivalent circuit is given below. As per the conduction of equivalent circuit, the output current expression of mode I is given as follows.

$$I_o = I_s - \frac{1}{V_s}\left(r_{o(1)} + j\omega\left(\frac{V_o T_D}{I_{in(max)}\left(1+\frac{\pi(a-1)}{2}\right)}\right) + \frac{1}{j\omega}\left(\frac{\left(V_o\left(1+\frac{\pi(a-1)}{2}\right)\right)}{I_{in(max)} T_D (a-1)^2}\right)\right) \quad (5)$$

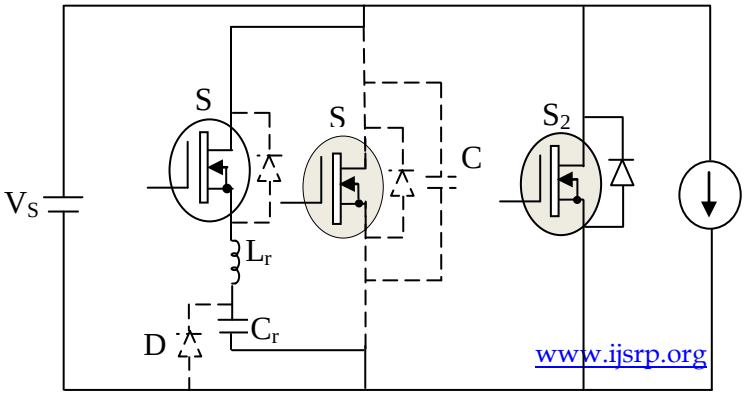

Figure 2: Equivalent Circuit of Mode I.

Mode II:

In mode II, the auxiliary circuit diodes are not conducted but, the MOSFET S_1 *and* S_2 are ZCS. Also, the resonant capacitor and resonant inductor are activated. The main circuit components go to ZVS. The current capacitor across the main circuit is not charged. The equivalent circuit model of mode II operation is given below. From the equivalent circuit model, the output current I_o expression is developed and it is given as follows.

(6)

$$I_o = I_s - \frac{1}{V_s}\left(r_{o(1)} + r_{o(2)} + j\omega\left(\frac{V_o T_D}{I_{in(max)}\left(1+\frac{\pi(a-1)}{2}\right)}\right) + \frac{1}{j\omega}\left(\frac{\left(V_o\left(1+\frac{\pi(a-1)}{2}\right)\right)}{I_{in(max)} T_D (a-1)^2}\right)\right)$$

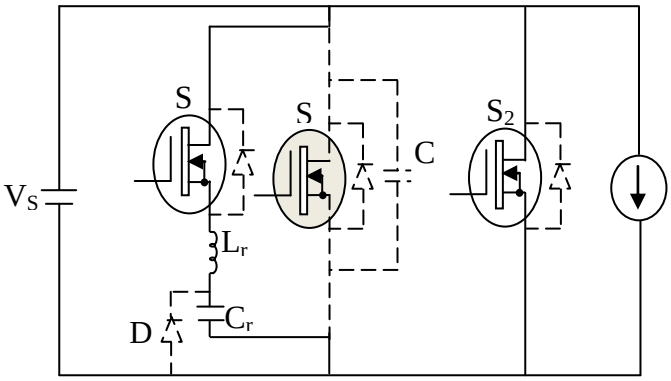

Figure 3: Equivalent Circuit of Mode II.

Mode III:

In mode III, the auxiliary circuit diodes are not conducted but, the MOSFET S_1 is ZCS and the MOSFET S_2 is ZVS. Also, the resonant capacitor and resonant inductor are activated. The main circuit MOSFET goes to ZVS and the MOSFET diode is conducted. The current source capacitor across the main circuit is not charged. The equivalent circuit model of mode III operation is given below. From the equivalent circuit model, the output current I_o expression is developed and it is given as follows.

$$I_o = I_s - \frac{1}{V_s}\left(r_{o(1)} + j\omega\left(\frac{V_o T_D}{I_{in(max)}\left(1+\frac{\pi(a-1)}{2}\right)}\right) + \frac{1}{j\omega}\left(\frac{\left(V_o\left(1+\frac{\pi(a-1)}{2}\right)\right)}{I_{in(max)} T_D (a-1)^2}\right)\right)$$

(7)

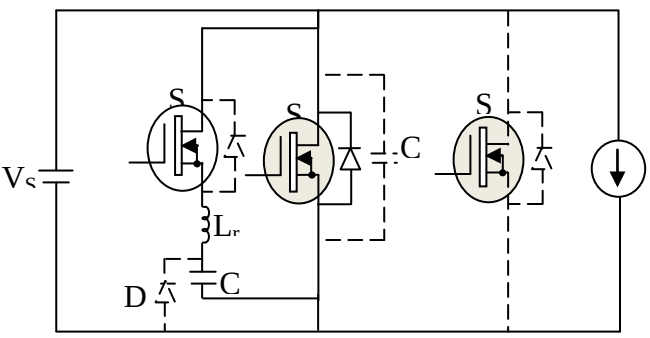

Figure 4: Equivalent Circuit of Mode III.

Mode IV:

In mode IV, the auxiliary circuit diodes are not conducted but, the MOSFET S_1 is ZCS and the MOSFET S_2 is ZVS. Also, the resonant capacitor and resonant inductor are activated. The main circuit MOSFET goes to ZCS and the MOSFET diode is not conducted. The current source capacitor across the main circuit is not charged. The equivalent circuit model of mode IV operation is given below. From the equivalent circuit model, the output current I_o expression is developed and it is given as follows.

$$I_o = I_s - \frac{1}{V_s}\left(r_o + r_{o(1)} + j\omega\left(\frac{V_o T_D}{I_{in(max)}\left(1+\frac{\pi(a-1)}{2}\right)}\right) + \frac{1}{j\omega}\left(\frac{\left(V_o\left(1+\frac{\pi(a-1)}{2}\right)\right)}{I_{in(max)} T_D (a-1)^2}\right)\right)$$

(8)

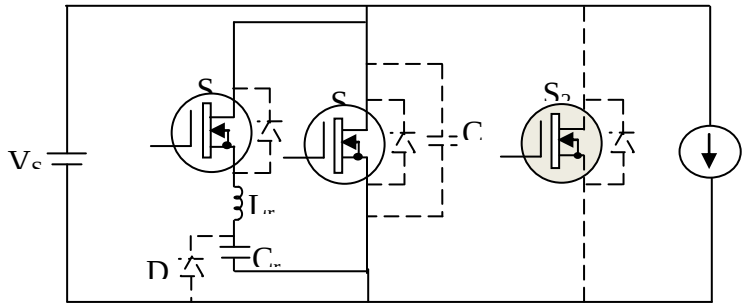

Figure 5: Equivalent Circuit of Mode IV.

Mode V:

In mode V, the auxiliary circuit MOSFET diodes one is conducted and other is not conducted but, the MOSFET S_1 and S_2 are ZVS. Also, the resonant capacitor and resonant inductor are activated. The main circuit MOSFET goes to ZCS and the MOSFET diode is not conducted. The current source capacitor across the main circuit is not charged. The equivalent circuit model of mode V operation is as follows. From, the equivalents circuit the model, the output current I_o expression is developed and it is given as follows.

$$I_o = I_s - \frac{1}{V_s}\left(r_o + j\omega\left(\frac{V_o T_D}{I_{in(max)}\left(1+\frac{\pi(a-1)}{2}\right)}\right) + \frac{1}{j\omega}\left(\frac{\left(V_o\left(1+\frac{\pi(a-1)}{2}\right)\right)}{I_{in(max)} T_D (a-1)^2}\right)\right)$$

(9)

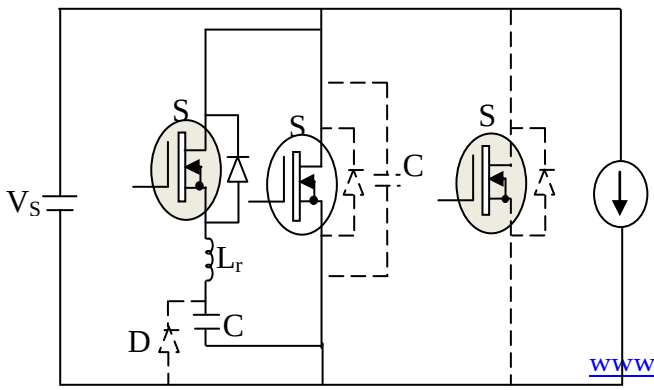

Figure 6: Equivalent Circuit of Mode V.

Mode VI:

In mode VI, the auxiliary circuit MOSFET diodes are not conducted, the MOSFET S_1 and S_2 are ZVS. Also, the resonant capacitor and resonant inductor are inactivated. The main circuit MOSFET goes to ZCS and the MOSFET diode is not conducted. The current source capacitor across the main circuit is not charged. The equivalent circuit model of mode VI operation is as follows. From the equivalent circuit model, the output current I_o expression is developed and it is given as follows.

$$I_o = I_s - \frac{r_o}{V_s} \quad (10)$$

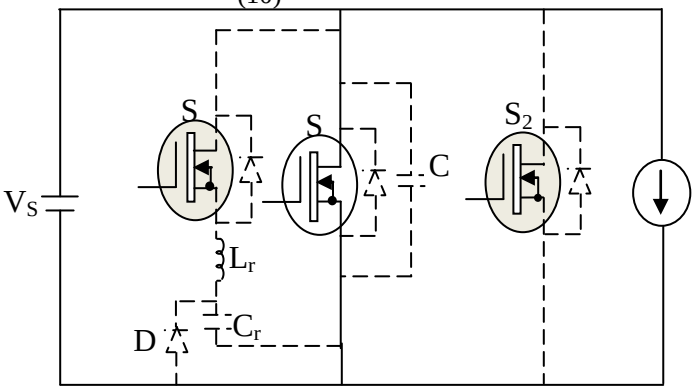

Figure 7: Equivalent Circuit of Mode VI.

Mode VII:

In mode VII, the auxiliary circuit MOSFET diodes are not conducted, the MOSFET S_1 and S_2 are ZVS. Also, the resonant capacitor is activated and resonant inductor is inactivated. Due to the reason, the auxiliary circuit diode is conducted. The main circuit MOSFET goes to ZVS and the MOSFET diode is not conducted. The current source capacitor across the main circuit is not charged. The equivalent circuit model of mode VII operation is as follows. From the equivalent circuit model, the output current I_o expression is developed and it is given as follows.

$$I_o = I_s - \frac{1}{V_s}\left(\frac{1}{j\omega}\left(\frac{\left(V_o\left(1+\frac{\pi(a-1)}{2}\right)\right)}{I_{in(max)}T_D(a-1)^2}\right)\right) \quad (11)$$

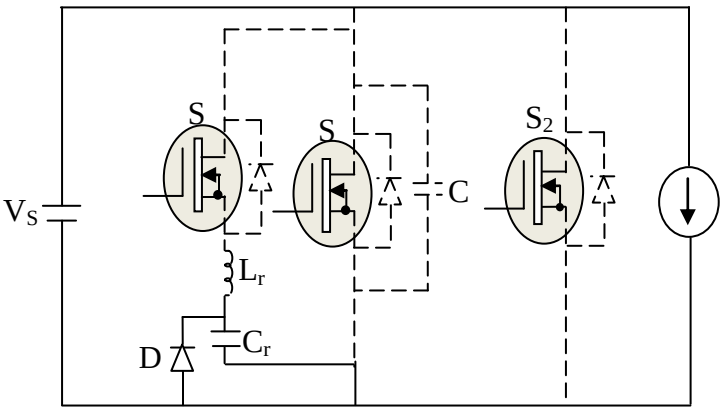

Figure 8: Equivalent Circuit of Mode VII.

Mode VIII:

In mode VIII, the auxiliary circuit MOSFET diodes are not conducted; the MOSFET S_1 is ZVS and MOSFET S_2 is ZCS. Also, the resonant capacitor and resonant inductor are inactivated. The main circuit MOSFET goes to ZVS and the MOSFET diode is not conducted. The current source capacitor across the main circuit is not charged. The equivalent circuit model of mode VIII operation is as follows. From the equivalent circuit model, the output current I_o expression is developed and it is given as follows.

$$I_o = I_s - \frac{r_{o(2)}}{V_s} \quad (12)$$

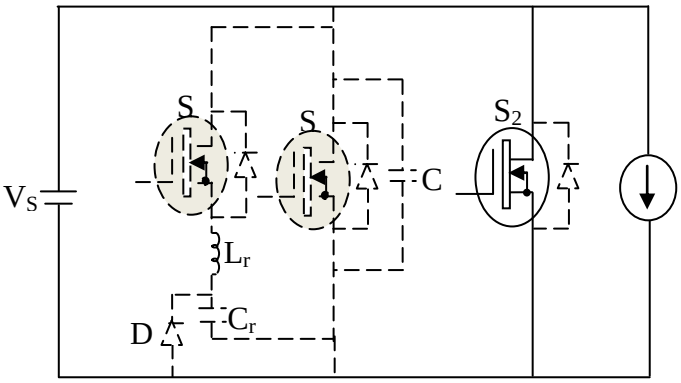

Figure 9: Equivalent Circuit of Mode VIII.

IV. Results and Discussion

The proposed synchronous DC-DC cuk converter was designed and simulated in MATLAB working platform. Then, the performance of synchronous cuk converter was tested with photovoltaic renewable energy system. The simulink model of synchronous cuk converter and the simulink model of cuk converter with photovoltaic system are illustrated in Fig.10 and Fig 11 respectively. From the model, the main MOSFET output voltage, and the output current performance are given in Figure 14 and 15 respectively. The V-P characteristics and V-I characteristics of PV system are illustrated in Figure 12 and 13. The implementation parameters of the proposed model are tabulated as follows.

Table I: Implementation Parameters.

Component	Parameters	Values
PV System	Short circuit current (I_{sc})	5.45A
	Open circuit voltage (V_{oc})	22.2V
	Current at P_{max}	4.95A

	Voltage at P_{max}	17.2V
MOSFET	FET resistance (R_{on})	0.1 Ohms
	Internal diode resistance (R_d)	0.01 Ohms
	Snubber resistance (R_s)	1e5 Ohms
	Resonant capacitor (C_r)	0.2$^{\mu}$F
	Resonant Inductor (L_r)	200nH
	Series Capacitor (C_s)	0.05nF

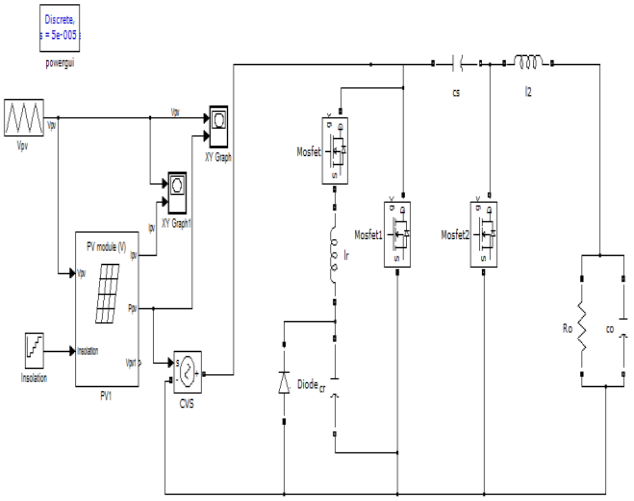

Figure 10: Simulink model of synchronous cuk converter with PV system.

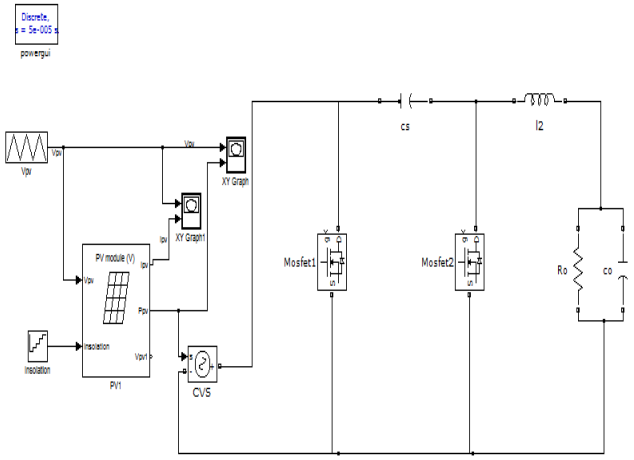

Figure 11: Simulink model of cuk converter with PV system.

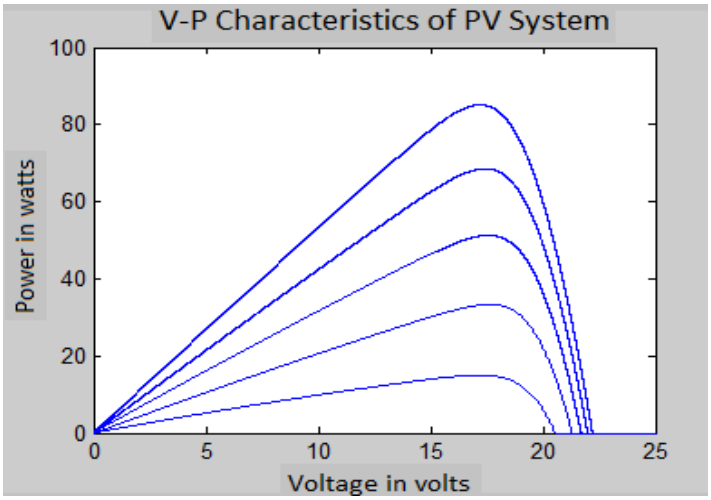

Figure 12: Performance of V-P of PV system.

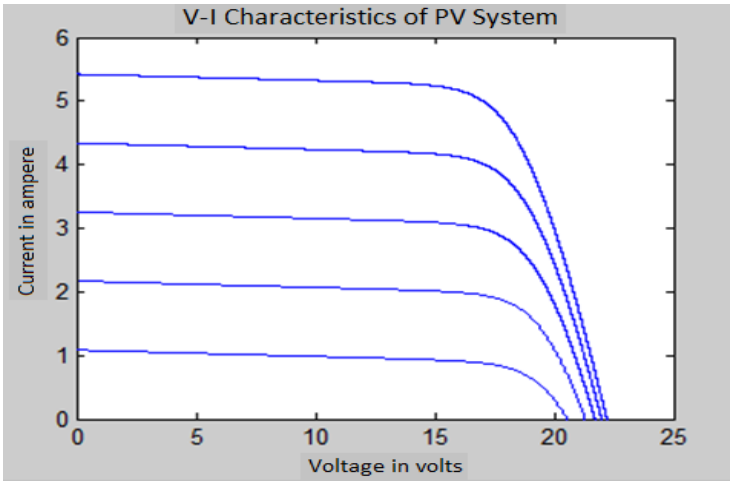

Figure 13: Performance of V-I of PV system.

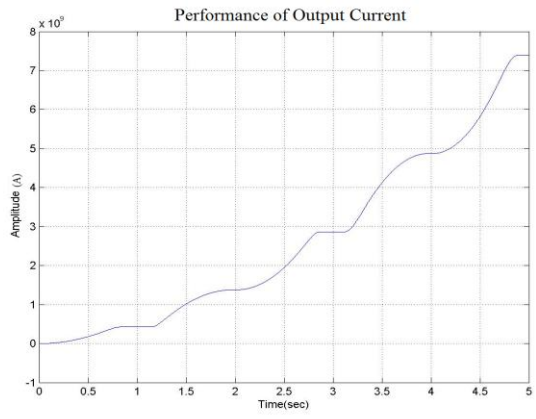

Figure 14: Performance of output current of proposed cuk converter.

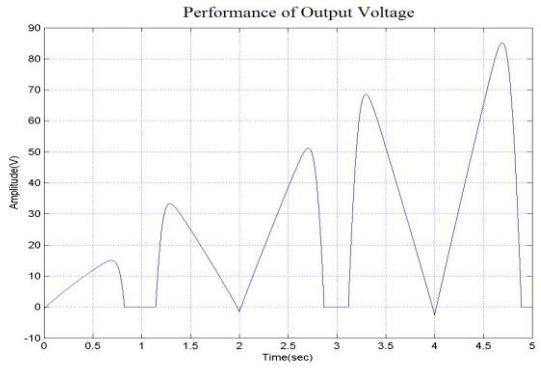

Figure 15: Performance of output voltage of proposed cuk converter.

From the above performances, the output voltage and output current of cuk converter are evaluated at different simulation period. According to the simulation period variations, the output power of the photovoltaic system is varied. Also, the output power of the proposed cuk converter is evaluated. The evaluated values are tabulated as following them (Table II). Similarly, the output current, voltage and power of cuk converter is evaluated using the model which represented in Figure 11.

Table II: Output voltage, current and power of synchronous cuk converter.

Time in sec	Output voltage in volts	Output current in amp	Output power in watts
T=1	15	0.5	7.5
T=2	34	1.5	51
T=3	52	2.8	145
T=4	68	4.8	326.4
T=5	85	7.4	629

In Table II, the voltage (V_o) and current (I_o) are calculated from figure 5 and 6. Using these calculated values, the output power is calculated $(P_o = V_o * I_o)$. Then the converter efficiency of both proposed synchronous cuk converter and cuk converter are calculated. The converter efficiency expression is given as following them.

$$Converter\ efficiency = \frac{P_o}{(P_o + coverter\ losses)} \times 100$$

The converter losses are varied in both synchronous cuk converter and cuk converter. In proposed synchronous cuk converter, the converter loss is 190 mW (0.19W). The converter loss of cuk converter is 445 mW (0.445W). These converter losses are based on the main MOSFET switching time. From the analyzed values, the following performances are obtained. The performance of synchronous cuk converter output power, performance of converter efficiency and performance of efficiency deviation are illustrated in Figure 16, 17 and 18 respectively. Then, the efficiency deviation of proposed converter is calculated by the following expression.

$$Efficiency\ deviation = \frac{Efficiency(\ synchronous\ cuk\ converter - \ cuk\ converter)}{synchronous\ cuk\ converter}$$

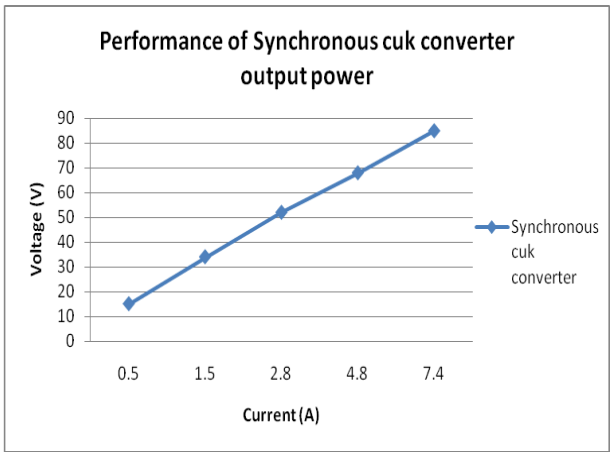

Figure 16: Performance of synchronous cuk converter output power.

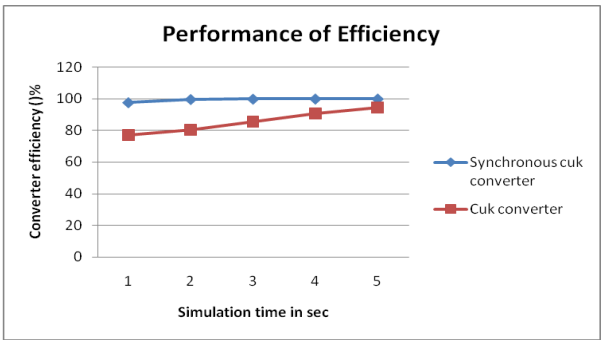

Figure 17: Performance of converter efficiency.

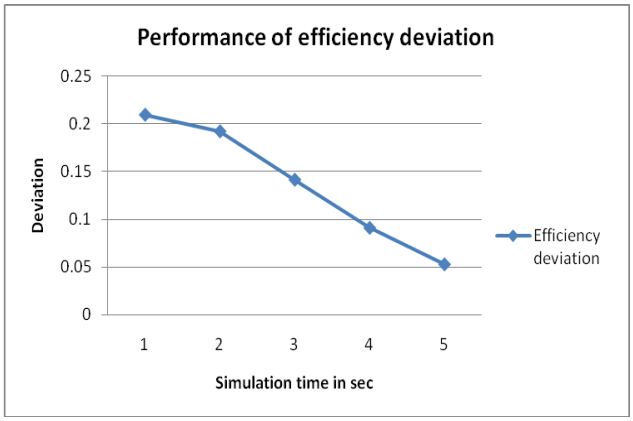

Figure 18: Performance of efficiency deviation.

From the comparative analysis, it is revealed that the proposed synchronous cuk converter is better when compared to the cuk converter. The proposed converter efficiency is deviated more than the cuk converter. Hence, the proposed synchronous cuk converter is better than the cuk converter for the photovoltaic application.

V. Conclusion

The proposed synchronous cuk converter was simulated in MATLAB simulation platform and the output performance was evaluated. Then, the mode of operation of proposed converter was analyzed by the operating condition of auxiliary and main circuit. From the eight operating mode circuit, the output currents were calculated. For evaluating the output performance, the proposed synchronous cuk converter output was tested with one PV system. From the testing results, the output power of the synchronous converter, the converter efficiency, and the efficiency deviation were analyzed. The analyses showed that the proposed synchronous cuk converter was better when compared to cuk converter.

References

[1] Assad Abu-Jasser, "A Stand-Alone Photovoltaic System, Case Study: A Residence in Gaza", Journal of Applied Sciences in Environmental Sanitation, Vol.5, No.1, pp.81-91, 2010

[2] A. Daoud and A. Midoun, "Fuzzy Control of a Lead Acid Battery Charger", Journal of Electrical Systems, Vol.1, No.1, pp.52-59, 2005

[3] R. Hosseini, N. Hosseini and H. Khorasanizadeh, "An experimental study of combining a photovoltaic system with a heating system", World Renewable Energy Congress, Vol.8, pp.2993-3000, 2011

[4] Mohamed Azab, "A New Maximum Power Point Tracking for Photovoltaic Systems", International Journal of Electrical and Electronics Engineering, Vol.3, No.11, pp.702-705, 2009

[5] M. Gohul, T. Jayachandran, A. Mohamed Syed Ali, T.G. Raju, N. Santhosh Kumar and M.R. Saravanan, "A New Design of Grid Tie Inverter for a Grid Interactive Solar Photovoltaic Power Generation – An Innovative Option for Energy Conservation & Security", International Journal of Electronics & Communication Technology, Vol.2, No.3, pp.161-166, 2011

[6] Klimis Ch. Karasavvas, "Modular simulation of a hybrid power system with diesel, photovoltaic inverter and wind turbine generation", Journal of Engineering Science and Technology Review, Vol.1, pp.38-40, 2008

[7] Jong-Pil Leey, Byung-Duk Min, Tae-Jin Kim, Dong-Wook Yoo and Ji-Yoon Yoo, "Input-Series-Output-Parallel Connected DC/DC Converter for a Photovoltaic PCS with High Efficiency under a Wide Load Range", Journal of Power Electronics, Vol.10, No.1, pp.9-13, January 2010

[8] Diary R. Sulaiman, Hilmi F. Amin and Ismail K. Said, "Design of High Efficiency DC-DC Converter for Photovoltaic Solar Home Applications", Journal of Energy and Power, 2010

[9] Rym Marouani, Kamel Echaieb and Abdelkader Mami, "New Alternative of Design and Control for Three-Phase Grid-Connected Photovoltaic System", European Journal of Scientific Research, Vol.55, No.1, pp.37-45, 2011

[10] Athimulam Kalirasu and Subharensu Sekar Dash, "Simulation of Closed Loop Controlled Boost Converter for Solar Installation", Serbian Journal of Electrical Engineering, Vol.7, No.1, pp.121-130, May 2010

[11] T.Chaitanya, Ch.Saibabu and J.Surya Kumari, "Modeling and Simulation of PV Array and its Performance Enhancement Using MPPT (P&O) Technique", International Journal of Computer Science & Communication Networks, Vol.1, No.1, pp.9-16, October 2011

[12] T. Mrabti, M. El Ouariachi, R. Malek, Ka. Kassmi, B. Tidhaf, F. Bagui, F. Olivie and K. Kassmi, "Design, realization and optimization of a photovoltaic system equipped with analog maximum power point tracking (MPPT) command and detection circuit of the dysfunction and convergence the system (CDCS)", International Journal of the Physical Sciences, Vol.6, No.35, pp.7865-7888, 2011

[13] M.SubbaRao, Ch.Sai Babu and S.Satynarayana, "Analysis and Control of Double-Input Integrated Buck-Buck-Boost Converter For Hybrid Electric Vehicles", International Journal of Advances in Engineering & Technology, Vol.1, No.4, pp.40-46, 2011

[14] G.shasikala, R.Chandralekha and C.Sasikala, "High Power Luo Converter With Voltage Lift For Stand Alone Photovoltaic System", International Journal of Advanced Engineering Sciences and Technologies, Vol.10, No.1, pp.37-41, 2011

[15] Elzbieta Szychta, "Multiresonant ZVS CUK Converter", Journal of Electrical Power Quality and Utilization, Vol.XII, No.2, pp.95-101, 2006

[16] C.K.Tse, Y.S.Lee and W.C.So, "An Approach to Modelling DC-DC Converter Circuits Using Graph Theoretic Concepts", International Journal of Circuit Theory and Application, Vol.21, pp.371-384, 1993

[17] Wael Salah, Soib Taib and Anwar Al-Mofleh, "Development of Multistage Converter for Outdoor Thermal Electric Cooling (TEC) Applications", Jordan Journal of Mechanical and Industrial Engineering, Vol.4, No.1, pp.15-20, 2010

[18] Y. Fuad, W. L. de Koning and J. W. van der Woude, "Pulse-width modulated d.c.–d.c. converters", International Journal of Electrical Engineering Education, Vol.38, No.1, pp.54-79, 2001

[19] I. Daho, D. Giaouris, S. Banerjee, B. Zahawi and V. Pickert, "Fast-Slow Scale Bifurcation in Higher Order Open Loop Current-Mode Controlled DC-DC Converters", International Federation of Automatic Control, Vol.2, No.1, 2009

[20] Jian Sun, Daniel M. Mitchell, Matthew F. Greuel, Philip T. Krein and Richard M. Bass, "Averaged Modeling of PWM Converters Operating in Discontinuous Conduction Mode", IEEE Transactions on Power Electronics, Vol.16, No.4, pp.482-492, July 2001

[21] Yu Kang Lo, , Huang-Jen Chiu, Ting-Peng Lee, Irwan Purnama and Jian-Min Wang, "Analysis and Design of a Photovoltaic System DC Connected to the Utility With a Power Factor Corrector", IEEE Transactions on Industrial Electronics, Vol.56, No.11, pp.4354-4362, November 2009

[22] Ho-sung Kim, Jong-Hyun Kim, Byung-Duk Min, Dong-Wook Yoo and Hee-Je Kim, "A highly efficient PV system using a series connection of DC–DC converter output with a photovoltaic panel", Renewable Energy, Vol.34, pp.2432–2436, 2009

[23] Athimulam Kalirasu and Subharensu Sekar Dash, "Simulation of Closed Loop Controlled Boost Converter for Solar Installation", Serbian Journal of Electrical Engineering, Vol.7, No.1, pp.121-130, May 2010

[24] Arun K. Verma, Bhim Singh and S.C Kaushik, "An Isolated Solar Power Generation using Boost Converter and Boost Inverter", International Journal of Engineering and Information Technology, Vol.2, No.2, pp.101-108, 2010

[25] M. Vaigundamoorthi and R. Ramesh, "ZVS-PWM Active-Clamping Modified Cuk Converter Based MPPT for Solar PV Modules", European Journal of Scientific Research, Vol.58, No.3, pp.305-315, 2011

[26] A.Kalirasu and S.S.Dash, "Modeling and Simulation of Closed Loop Controlled Buck Converter for Solar Installation", International Journal of Computer and Electrical Engineering, Vol.3, No.2, pp.206-210, April 2011

[27] W.M.Utomo, Z.A. Haron, A. A. Bakar, M. Z. Ahmad and Taufik, "Voltage Tracking of a DC-DC Buck-Boost Converter Using Neural Network Control", International Journal of Computer Technology and Electronics Engineering, Vol.1, No.3, pp.108-113, 2011

Authors

First Author – K,Kavitha, Department of ECE, Vivekanandha Institute of Engineering and Technology for Women, Tiruchengode, Tamilnadu, India

Second Author – Dr. Ebenezer Jeyakumar, Director (Academics), Sri Ramakrishna Engineering College, Ciombatore, Tamilnadu, India